CHAPTER V
PREPARATION AND CHARACTERIZATION OF CHITIN WHISKER-REINFORCED SILK FIBROIN NANOCOMPOSITE SPONGES

5.1 Abstract

For highly porous form such as sponges or scaffolds, the induction of the β-sheet formation to make the water-stable materials usually results in their high shrinkage leading to a difficulty in controlling shape and size of materials. Thus, the objective of this study was to improve dimensional stability of silk fibroin sponge by incorporating chitin whisker as nanofiller. Chitin whiskers exhibited the average length and width of 427 and 43 nm, respectively. Nanocomposite sponges at chitin whiskers to silk fibroin weight ratio (C/S ratio) of 0, 1/8, 2/8, or 4/8 were prepared by using a freeze-drying technique. The dispersion of chitin whiskers embedded in the silk fibroin matrix was found to be homogeneous. The presence of chitin whiskers embedded into silk fibroin sponge not only improved its dimensional stability but also enhanced its compression strength. Regardless of the chitin whisker content, SEM micrographs showed that all samples possessed an interconnected pore network with an average pore size of 150 μm. To investigate the feasibility of the nanocomposites for tissue engineering applications, L929 cells were seeded onto their surfaces, the results indicated that silk fibroin sponges both with and without chitin whiskers were cytocompatible. Moreover, when compared to the neat silk fibroin sponge, the incorporation of chitin whisker into the silk fibroin matrix was found to promote cell spreading.

Keyword: Silk fibroin; Chitin whisker; Nanocomposite; Scaffold

5.2 Introduction

Silk fibers from the silkworm *Bombyx Mori* have been used commercially as biomedical sutures for decades but some biocompatibility problems have been reported during the past 20 years [1-3]. However, after silk sericin is properly extracted, silk fibers and regenerated silk fibroin films exhibit comparable biocompatibility *in vitro* and *in vivo* with other commonly used biomaterials such as polylactic acid and collagen [1,4]. Regenerated silk fibroin is also biodegradable [5-7], and a number of cells, e.g. L929 cells [8], endothelial cells [9], keratinocytes, osteoblasts [10], fibroblasts [10,11], bone marrow stromal cells [12], and bone marrow-derived mesenchymal stem cells [13], have been shown to grow well on its surface. Because of its high cytocompatibility, the regenerated silk fibroin is an interesting scaffolding biomaterial applicable for a wide range of target tissues.

Before actual use, the regenerated silk fibroin requires post-treatment in order to induce the conformation transition from random coil to β-sheet formation to attain a water-stable material. Post-treatments of silk fibroin can be done by using an aqueous alcohol solution [14], thermal annealing [15] or physical stretching [7]. Among them, the method of annealing with solvents is much more widely used than others because it is simple and performed under mild condition; however, this transition induction causes the shrinkage of the material leading to its poor dimensional stability, especially for highly porous material. In this study, silk fibroin sponges also show a relatively low strength. Normally, materials must have sufficient mechanical integrity to resist handling during implantation and *in vivo* loading. Therefore, these two important limitations of silk fibroin need to be solved.

In the plastic industry, the use of inorganic fillers has been a common way to improve mold shrinkage, thermal and mechanical properties of thermoplastics. The effect of filler on the mechanical and other properties of the composites depend greatly on its shape, particle size, aggregated size, surface characteristics, and degree of dispersion. Generally, the mechanical properties of the composites filled with micron-sized filler particles are inferior to those filled with nanoparticles of the same filler

[16,17]. Intuitively, the adaptation of knowledge in thermoplastic nanocomposite is expected to be useful for biomaterials.

It is known that the mechanical properties of the composites are strongly related to the aspect ratio of the filler particles. Based on this, the chitin whiskers, having a wide range of aspect ratios, i.e. 10 to 120, depending on types of sources, have been extensively studied as reinforcing nanofillers in recent years [18-23]. Chitin or poly(β(1-4)-N-acetyl-D-glucosamine) is one of the most abundant polysaccharides found in nature. It can be found in the skeletal materials of crustaceans, cuticles of insects, and cell walls of various fungi. Chitin is known to be cytocompatible [24-26] and biodegradable [27]. In addition, chitin whiskers have been successfully prepared from crab shells [19-21,28,29], squid pens [30], tubes of *Riftia pachyptila* tubeworms [18], and shrimp shells [22,23].

In this study, chitin whisker-reinforced silk fibroin nanocomposite sponges were fabricated using a freeze-drying technique. The presence of chitin whisker embedded in silk fibroin matrix was expected to improve their dimensional stability as well as the mechanical properties. The effect of the whisker content on the morphology of the sponges, and the interaction between chitin whisker and silk fibroin were also discussed. The dispersion of chitin whisker in fibroin matrix was investigated. In addition, the morphologies of L929 cells on silk fibroin sponges with and without chitin whisker were observed.

5.3 Experimental

5.3.1 Materials

Raw silk fiber, *Bombyx Mori*, was obtained from Queen Sirikit Sericulture Center, Saraburi Province (Thailand). Shell of *Penaeus merguiensis* shrimp was kindly supplied by Surapon Foods Public Co., Ltd (Thailand). All of the materials (analytical grade) were used as received.

5.3.2 Preparation of Chitin Whisker Suspension

After decalcification and deproteinization, the degree of deacetylation (DD) of the obtained chitin was determined by Fourier-transformed infrared spectroscopy (FTIR) following the method of Baxter *et al.* [31] and was found to be 20%.

The preparation of chitin whisker was modified from the method of Morin & Dufresne [18]. Briefly, chitin whisker suspension was prepared by hydrolyzing chitin flake (< 2 mm) with 3 N HCl at its boiling point (i.e. 104°C) for 6 hours under vigorous stirring. The ratio of 3 N HCl to chitin sample was 30 $cm^3 \cdot g^{-1}$. After acid hydrolysis, the suspension was diluted with distilled water, followed by centrifugation at 10,000·rpm for 10 min. This process was repeated three times. The suspension was then transferred to a dialysis bag and dialyzed in running water for 2 h and later in distilled water until the pH of the suspension became neutral. The dispersion of the whisker in the suspension was completed by ultrasonication treatment for 10 min. The suspension was refrigerated at 4°C prior to further use. The solid content of the as-prepared chitin whisker suspension was 4.63 wt%.

5.3.3 Preparation of Aqueous Silk Fibroin Solution

The raw silk fibers of *Bombyx mori* were boiled for 15 min in an aqueous solution of 0.05% Na_2CO_3. The boiling process was repeated two times to remove sericin. The fibers were then rinsed thoroughly with hot water and dried at 40°C overnight. After drying, the degummed silk fibers were dissolved in a solvent mixture of $CaCl_2$:Ethanol:H_2O (molar ratio = 1:2:8) at 78°C. The undissolved particle was filtered out using filter cloth. The filtrated solution was subsequently dialyzed in distilled water for 4 days by changing the media daily, followed by centrifugation at 10,000 rpm for 10 min. The as-prepared aqueous silk fibroin concentration was 6.32 wt%.

5.3.4 Preparation of Chitin Whisker-reinforced Silk Fibroin Sponges

The as-prepared chitin whisker suspension were added to distilled water to achieve a chitin whisker concentration at 0, 0.125, 0.25 or 0.50 wt% (a concentration based on the final volume including distilled water, chitin whisker suspension, and silk fibroin solution) with a volume of 8.42 ml. The suspensions were then treated by ultrasonication for 10 min. After the suspension was kept at 4°C for 10 min, 1.58 ml of 6.32 wt% aqueous silk fibroin solution was added to the suspension with slow mechanical stirring. The obtained chitin whisker/silk fibroin suspension was equivalent to chitin whiskers to silk fibroin weight ratio (C/S ratio) of 0, 1/8, 2/8, or 4/8. The mixture suspension was further stirred mechanically for 10 min before being poured with 1.6 ml into each well of a 24 multi-wells culture plate (COSTAR®, Corning Inc., NY, USA). The suspension was frozen at -40°C overnight under controlled cooling rate, followed by freeze-drying under vacuum condition of less than 10 Pa for 24 hours to obtain the nanocomposite sponges.

5.3.5 Methanol Treatment

The silk fibroin sponges both with and without chitin whiskers were immersed in an aqueous methanol solution at a concentration of 90% (v/v) for 10 min. After excessively washing with distilled water, the methanol-treated sponges were subsequently frozen at -40°C overnight under controlled cooling rate, followed by freeze-drying under vacuum condition of less than 10 Pa for 24 hours.

5.3.6 Characterization of Chitin Whisker-reinforced Silk Fibroin Samples

The volume of the sponges before and after methanol treatment was determined in order to calculate the percent shrinkage (i.e. shrinkage (%) = $(V_i - V_f)/V_i \times 100$; where V_i and V_f represent the volume of the sponges before and after methanol treatment, respectively). The sample number was five for each experimental group.

The compression test was performed for the dried sponges of the methanol-treated samples at room temperature on the Texture Analyzer (TA.XT2i,

England) at a crosshead speed of 0.5 mm/min. The compressive modulus was calculated from the initial slope of the linear portion of the stress–strain curve [32]. In order to eliminate the influence of additional weight of the sponges from mixing with chitin whiskers and the volume change after methanol treatment, the compressive modulus was then divided by the bulk density, namely the specific modulus [33]. The experiment was performed for four sponges per sample.

FTIR spectrophotometry was used to verify the chemical structure and conformation of the as-prepared silk fibroin sponge, methanol-treated sponges at various C/S ratios, and chitin whisker film. The measurements were carried out on a Thermo Nicolet Nexus 671 FT-IR (32 scans at a resolution of 4 cm^{-1}). A Mettler-Toledo differential scanning calorimetry (DSC) model 822e/400 was used to evaluate thermal properties of the methanol-treated silk fibroin sponges with and without chitin whisker, and the freeze-dried chitin whisker (about 3 mg) under N_2 atmosphere at a heating rate of 10 $K \cdot min^{-1}$ from 50 to 450°C.

The inner microstructure of the as-prepared silk fibroin sponges with and without chitin whisker, and the corresponding methanol-treated sponges was observed by a scanning electron microscope (SEM, JSM-5410LV, Jeol, Japan) at a voltage of 15 kV. The sponge was cut with a razor blade. The cross-section of the sponges was coated with gold on the ion sputter (SCD040, Lichtenstein) at 50 mTorr and 15 mA for 4 min.

The morphological appearance and sizes of the as-prepared chitin whiskers were observed using a JEOL JEM-1230 transmission electron microscope (TEM). Samples were prepared from a drop of a dilute chitin whisker suspension which was deposited and left to dry on a carbon coated copper grid. The dispersion of chitin whisker in the silk fibroin matrix was also observed with TEM by embedding the sponge at C/S ratio of 4/8 with Aradite resin. The sample was then cut to ultrathin sections (200 nm) and placed on a copper grid with a carbon coating. The observations were carried out at an accelerating voltage of 120 kV.

The universal hardness (H) of silk fibroin and chitin whisker/silk fibroin films at C/S ratio of 4/8 was carried out using Nanoscope (R) IV scanning probe

microscope (Veeco/Digital Instruments, CA) in a nano-indentation mode in order to investigate the influence of hardness on cell spreading. The diamond-tipped probe made a prescan to measure the surface profile. The probe then applied the force at a trigger threshold of 3 V (230 μN) onto the scanned film surfaces (spring constant of 291 N/m specified by the manufacturer). The hardness were calculated from $H = Force/A$, where A is the projected area at peak load.

5.3.7 Cells and Cell Culture

A cell line of L929 (ECACC Cat. No. 85011425) mouse connective tissue, which is a fibroblast-like cell, was cultured in Dulbecco's modified Eagle's medium (DMEM; Sigma-Aldrich, USA) supplemented with 10% fetal bovine serum (FBS, BIOCHROM AG), together with 100 units/ml penicillin (GIBCO) and 100 μg/ml streptomycin (GIBCO) at 37°C in a wet atmosphere containing 5% CO_2. When the cells reached 80% confluence, they were trypsinized with 0.25% trypsin containing 1 mM EDTA (GIBCO) and counted by a hemacytometer (Hausser Scientific, USA) before use in the experiments.

5.3.8 Cell Spreading Analysis

In these experiments, each prepared sponge was placed in a 24-well culture plate and sterilized by 70% ethanol solution for 30 min. Thereafter, it was washed twice with phosphate buffer saline (PBS, pH 7.4) and subsequently washed with culture media. Before cell seeding, 500 μl of culture medium was pipetted into each well of the 24-well plate. 1×10^5 of L929 cells were seeded into each well of the culture plate and allowed to attach to the methanol-treated silk fibroin and chitin whisker/silk fibroin sponges (at C/S ratio of 4/8) for 6 h or 24 h. After each sample was rinsed twice with PBS, they were fixed with 3% glutaraldehyde for 30 min, followed by two rinses with a 0.2 M phosphate buffer. Then the samples were dehydrated through a series of graded ethanol and subsequently dried in a critical point dryer with liquid CO_2. The samples were gold sputtered in a vacuum at 50 mTorr and 15 mA for 4 min.

Cell spreading was evidenced from SEM micrographs taken by a JSM-5410LV scanning electron microscope at a voltage of 15 kV. The cells that adopted a flattened, polygonal shape, with filopodia- and lamellipodia-like extensions were regarded as spreading cells. In contrast, the cells that resisted to washing and remained tethered to the surface were regarded as non-spreading cells. The percent cell spreading was quantified by dividing the number of spread cells by the total number of bound cells (N=100 cells) [34]. Standard deviations were calculated from two independent experiments.

5.3.9 Statistical Analysis

All the results were statistically analyzed by the unpaired Student's t-test and the result with $P<0.05$ was considered to be statistically significant. Data were expressed as the mean ± the standard deviation of the mean (SD).

5.4 Results and Discussion

5.4.1 Morphology and Size of Chitin Whiskers

As stated, several investigations indicated that the regenerated silk fibroin exhibited a number of prerequisites for tissue engineering scaffolds; however, the shrinkage of the regenerated silk fibroin after methanol treatment was scarcely concerned. Although there were some researchers who attempted to fabricate silk fibroin without methanol treatment, the proposed methods were restricted to the preparation of only the film using a very high concentration of silk fibroin (>8 wt%) [7,35]. However, a very interesting method to prepare an insoluble silk fibroin sponge without methanol treatment was proposed by the work of Kim *et al.* [36] who prepared the silk fibroin sponges via a salt leaching technique.

For commercially available products, type I Collagen-Glycosaminoglycan (CG) sponges are successfully being used to regenerate skin in burn patients; this material received FDA approval for clinical use in 1996. Porous CG sponges have been

primarily fabricated using a freeze-drying technique [37]. The structure of the sponge is controlled by the final temperature of freezing and the heat transfer processes associated with freezing. Furthermore, the formation of ice crystals within the suspension is influenced by both the rate of nucleation of ice crystals and the rate of heat and protein diffusion [38]. In this study, the chitin whisker-reinforced silk fibroin nanocomposite sponges were successfully prepared via a freeze-drying technique because chitin whisker suspension displayed the colloidal behavior and there was no precipitation of chitin whisker occurred during mixing with the silk fibroin solution.

Considering morphology and size of chitin whisker, Figure 5.1A is the TEM micrograph of a dilute suspension of chitin whisker from the acid hydrolysis of shrimp chitin. It was found that the suspension was composed of chitin fragments containing both individual microcrystals and aggregated microcrystals. The chitin fragments were consisted of slender rods with sharp points which had a broad distribution in size. The length of the chitin fragments ranged from 180 to 820 nm, while the width ranged from 8 to 74 nm. The average length (L) and width (d) of these whiskers were about 427 and 43 nm, respectively, and the average aspect ratio (L/d) was of 10. These dimensions are in the range of the previously reported values for chitin whiskers obtained from the same source of chitin (L=150 to 800 nm and d=5 to 70 nm [22,23]). However, the dimensions of chitin whiskers prepared from other sources having a wide range reported values such as crab shells (L=50 to 300 nm and d=6 to 8 nm [28]; L=100 to 600 nm and d=4 to 40 nm [19-21]; and L=100 to 650 nm and d=10 to 80 nm [29]) squid pens (L=50 to 300 nm and d= ~10 nm [30]), or *Riftia* tubes (L= 500 nm to 10 μm and d= ~18 nm [18]).

In addition, the chitin suspension exhibited colloidal behavior due to the presence of the positive charge on chitin whisker. The shrimp chitin used to prepare chitin whisker in this work had a degree of deacetylation of 20%. It implied that there were some amino groups over the surface of chitin whisker. At neutral pH, the number of protonated amino groups ($-NH_3^+$) on the surface of chitin whisker was slightly lower than that of amino groups ($-NH_2$) because pH of the suspension was higher than pKa of -

NH_2 (~6.4) [39]. However, the presence of the positive charge of the protonated amino groups on the whisker surface was sufficient enough to stabilize the colloidal behavior of the chitin suspension [40].

5.4.2 Dimensional Stability

In order to determine dimensional stability after methanol treatment, the changes in the volume of the silk fibroin sponges both before and after methanol treatment was measured. Figure 5.2 illustrates the percent shrinkage of silk fibroin sponges both with and without chitin whisker. It was found that the percent shrinkage of the silk fibroin sponges could be significantly reduced at all C/S ratios. In addition, the percent shrinkage decreased with an increasing of the whisker content and finally reached the plateau at C/S ratio of 2/8. Interestingly, at only C/S ratio of 1/8, the percent shrinkage of the sponges reduced appreciably from 35.7 to 16.0.

It is known that methanol treatment of silk fibroin induces the transition of random coil conformation to β-sheet structure which results in the shrinkage of materials. After incorporating chitin whisker into silk fibroin sponge, the shrinkage of the nanocomposite sponges was appreciably reduced. To explain the shrinkage reduction of the nanocomposite sponges, conformation of silk fibroin existent in the methanol-treated nanocomposite sponges had to be clarified whether the presence of chitin whisker inhibited or disrupted β-sheet formation of silk fibroin. Figure 5.3 illustrates the FTIR spectra of the as-prepared silk fibroin sponge, the methanol-treated sponges with various C/S ratios, and the chitin whisker film. The neat silk fibroin sponge before methanol treatment exhibited the characteristic absorption peaks which were assigned to the random coil conformation at 1648 (amide I), 1536 (amide II) and 1237 cm^{-1} (amide III) [41]. After the silk fibroin sponge was treated with methanol, the peaks of amide I and amide II were shifted to 1624 and 1516 cm^{-1}, respectively, and a new absorption shoulder was observed at 1697 and 1268 cm^{-1}, which are the characteristic absorptions of β-sheet form of silk fibroin [42]. For chitin whisker, the characteristic absorption

peaks of chitin whisker were presented at 1658, 1116 and 1075 cm^{-1}, which were assigned to amide I, secondary alcohol, and primary alcohol, respectively [43].

Considering the FTIR spectra of the nanocomposite, it is obvious that the sponges at all C/S ratios showed the characteristic absorption peaks of β-sheet structure at 1624, 1516 cm^{-1}, and the absorption shoulder at 1697 and 1268 cm^{-1}. In addition, the absorption peak of primary alcohol of chitin whisker at 1075 cm^{-1} also present and the intensity of this peak increased with an increasing of C/S ratio. Thus the presence of chitin whisker in silk fibroin sponge did not inhibit the β-sheet formation of silk fibroin after methanol treatment. This indicated that the reduction of the shrinkage of the nanocomposite sponges was not resulted from the inhibition of the β-sheet formation. Dissolution test of the sponges also confirmed the FTIR results, the as-prepared nanocomposite sponges could be dissolved within a few minutes after submerging in distilled water for all C/S ratios. In contrast, the methanol-treated nanocomposite sponges were stable in water regardless of C/S ratios.

Chen *et al.* [44] suggested that the low shrinkage during the curing of the epoxy resin-based nanocomposite was caused by the strong interfacial interactions between the resin and nanosilica fillers. In order to investigate the interaction between silk fibroin and chitin whisker, the thermal properties of silk fibroin and their nanocomposite samples might provide useful information. Figure 5.4 shows the DSC thermograms of the methanol-treated chitin whisker/silk fibroin sponges at different C/S ratios, and the freeze-dried chitin whisker within the temperature range of 50 to 450°C. Apparently, two different types of thermal transition were observed in these thermograms. It was postulated that the wide endothermic peak at temperature below 190°C was a result of the loss of moisture within the samples, while another peak at higher temperature region was caused by the thermal decomposition of the samples.

According to Figure 5.4A, the decomposition temperature of neat silk fibroin appeared to be at the broader endothermic peak of 287°C and at the sharper endothermic peak of 304°C. The presence of the whisker at C/S ratio of 1/8 (see Figure 5.4B) induced the lowering of the sharp peak of the decomposition temperature from

304 to 298°C with the change in thermal transition from the rough to smooth curve but the wide endothermic peak of the decomposition temperature (288°C) was still similar. The further increase in the amount of chitin whisker (see Figures 5.4C and 5.4D) resulted in the absence of the sharp endothermic peak of the decomposition temperature. Analogous to C/S ratio of 1:8, the broad endothermic peak of the decomposition temperature (287°C) was still unchanged. By careful consideration of the thermograms present in Figures 5.4C and 5.4D (belonging to the nanocomposite with C/S ratio of 2/8 and 4/8), there was a new exothermal curve, which could not be observed in the thermograms of both neat silk fibroin and chitin whisker, due to the shift of the baselines in the range of 385 to 415°C. It should be noted that the decomposition of the chitin whisker caused the curve shifting (exothermic) of the baseline in the temperature range of 260 to 410°C (see Figure 5.4E).

Compared to the neat silk fibroin and chitin whisker, the noticeable change in the thermal decomposition behavior of the nanocomposites might imply to the interfacial interactions (mainly hydrogen bonding) forming between polar groups present in the chemical structures of silk fibroin and chitin whisker in the nanocomposite sponges. These interactions restricted the mobility of silk fibroin chains and also reduced inter- and intra-molecular interactions between silk fibroin chains. Therefore, the shrinkage of the silk fibroin nanocomposite sponges after methanol treatment could be reduced.

In addition, a short single crystal fiber, i.e. chitin whisker, is a highly crystalline material so its volume is still unchanged after methanol treatment. Hence, the incorporation of dimension-stable fillers into the matrix resulted in a reduction in the percent shrinkage of the sponges, which also decreased with an increasing amount of the stable filler. These results are analogous to the study of Hokugo *et al.* [32] who demonstrated that the incorporation of poly(glycolic acid) micro-fiber (whose volume was not changed during submersion in the culture media) into fibrin sponges resulted in the reduction of the percent shrinkage compared to the neat fibrin sponge, and the percent shrinkage of the sponge also decreased with increasing of the fiber content.

5.4.3 Compression Test

Typically, the purposes or advantages of the incorporation of the nanofillers into the matrix are to mimic the target organ component [45,46], to enhance the biological reponses, i.e. cell adhesion, proliferation [46] or biodegradation rate [47], and/or frequently to promote the mechanical properties [45,47,48].

The specific moduli of the methanol-treated silk fibroin sponges with and without chitin whiskers are shown in Table 5.1. The specific modulus was calculated by dividing the compressive modulus by the bulk density. Apparently, although the specific modulus of the methanol-treated nanocomposite at C/S ratio of 1/8 was comparable to that of the neat silk fibroin sponges, the specific moduli of those at C/S ratio of 2/8 and 4/8 were statistically significant higher by 2.6 and 7.5 orders of magnitude, respectively, when compare to that of the control sample. Favier *et al.* [49,50] found that when cellulose whisker content was reached in percolation threshold, the mechanical properties of the cellulose whisker-reinforced polymer nanocomposite films were substantially enhanced. They demonstrated that the substantial enhancement of the mechanical properties was caused by the hydrogen-bonding between the whiskers that hold the percolating network of the whiskers. They further suggested that good dispersion of the whiskers was also another important factor that promoted the mechanical properties.

Figure 5.1B is the TEM micrograph which illustrates the homogeneous dispersion of chitin whiskers embedded in the silk fibroin matrix. The morphology of chitin whisker exhibited the individual microcrystals without aggregation. Embedded chitin whisker displayed the width in the range of 7 to 68 nm, while its average was 21 nm which correlated to the size of bare chitin whisker in section 5.4.1 even the average was slightly lower. Therefore, when incorporating chitin whisker into silk fibroin at a suitable ratio, the compressive properties of the sponges were substantially improved. Note that the TEM micrograph displays only the perpendicular and tilt cross-section of

the whiskers without showing the entire rod of the whisker because the TEM micrograph was taken from the ultrathin sample with the thickness of 200 nm.

5.4.4 Morphological Appearance of Nanocomposite Sponges

For tissue engineering applications, the cellular structure of the sponge is one of the most important factors determining whether regeneration of a new tissue is successful or not. In general, the cellular structure of the sponge must be designed to satisfy a number of requirements, e.g. the pore size must be in a critical range (usually 100-200 μm) and the porosity must be interconnected to allow the ingrowth of cells, vascularization and the diffusion of nutrients [37].

Figure 5.5 is the SEM micrographs of silk fibroin sponges with and without chitin whisker after immersing in a 90% (v/v) aqueous methanol solution for 10 min in a comparison with the as-prepared sponge. Regardless of chitin whisker content, an interconnected pore network was observed with an average pore size of 150 μm for the sponges both before (see Figures 5.5A, 5.5B, 5.5C and 5.5D) and after methanol treatment (see Figures 5.5E, 5.5F, 5.5G and 5.5H), despite the fact that a contraction occurred in all methanol-treated samples especially a substantial contraction of the methanol-treated silk fibroin sponges (viz. the percent shrinkage of the sponges was 35.7, see Figure 2). In a separated experiment, all of the dried methanol-treated samples could absorb and sink in distilled water within a few seconds after dropping. This observation confirmed the presence of an interconnected pore network in the materials, corresponding to the SEM observation.

5.4.5 Morphological Appearance of Cell Adhesion and Analysis of Cell Spreading

Undoubtedly, both neat silk fibroin and chitin are not cytotoxic. However, the morphology of the attached cells on the sponges had to be observed in order to confirm the feasibility of the chitin whisker-reinforced silk fibroin nanocomposite sponges for tissue engineering applications.

Figure 5.6 shows the SEM micrographs of L929 cells cultured on the methanol-treated silk fibroin and chitin whisker/silk fibroin sponges at C/S ratio of 4/8. SEM micrographs revealed the cell morphology and interaction between cells and sponges. At 6 hours of cultivation, it was observed that the cells could attach on both types of sponges with their filopodia. The cells also exhibited different shapes, including flattening, typical elongated fibroblast cell shapes, and spherical shapes on both types of sponge (see Figures 5.6A and 5.6C). At 24 hours of cultivation (see Figures 5.6B and 5.6D), the number of cells with extended filopodia was observed to be relatively higher (compared to at 6 hours) and they showed a typical cell morphology on both types of sponges.

Interestingly, an observed number of flattened cells on the methanol-treated chitin whisker/silk fibroin sponges were higher than that on the methanol-treated neat silk fibroin sponges. At this point, it was interested to quantify the percent cell spreading on both types of matrix to determine the influence of the incorporated chitin whisker on cell spreading. Cell spreading analysis revealed that there was no statistically significant difference between both types of the substrates at 6 hours of cultivation; however, the cells could attach to the chitin whisker/silk fibroin sponges with significantly higher percent cell spreading compared to the neat silk fibroin sponges at 24 hours of cultivation (see Figure 5.7). It should be noted that the percent cell spreading at 24 hours of cultivation on chitin whisker/silk fibroin sponges was almost twice (61%) compared to that on the neat silk fibroin sponges (31%).

From literature, a number of physicochemical surface properties; surface free energy [51, 52], surface charge [53], surface chemistry [54], and surface topography [55], have been shown to affect cell spreading. Recently, the mechanical properties of substrates have been demonstrated to affect cell spreading as well. Pelham and Wang [56] prepared substrates from polyacrylamide sheets with different crosslinking densities and the surfaces of the prepared substrates were coated with type I collagen in order to vary the rigidity while maintaining the chemical environment. They found that cells on flexible substrates showed reduced spreading when compared to that on rigid substrates.

Fereol *et al.* [57] also found similar results even with substrates having different surface chemistries.

Generally, the incorporation of rigid fillers into the polymeric matrixes could improve their rigidity or hardness. In the present study, the incorporation of chitin whisker at C/S ratio of 4/8 significantly enhanced the rigidity of the silk fibroin matrix as compared between the universal hardness of the silk fibroin films with and without chitin whisker; 1.55±0.21 and 1.05±0.12 GPa, respectively. Therefore, the enhancement of the rigidity of silk fibroin films by incorporation of the chitin whisker might cause better cell spreading.

It could be concluded that both methanol-treated silk fibroin and chitin whisker/silk fibroin sponges exhibited the absence of cytotoxicity because the cells attached on the substrates showed the normal cell morphology. In addition, the incorporation of chitin whiskers into the silk fibroin matrix enabled the significant promotion of the percent cell spreading of the L929 cells.

5.5 Conclusion

Because of the colloidal behavior of the chitin whisker and no observation of a precipitation after mixing chitin whisker with silk fibroin, a freeze-drying technique can be used for fabrication of the sponge form and produced the materials having a pore size in a critical range with interconnecting pore network. The incorporating chitin whisker into the silk fibroin matrix not only promoted the dimensional stability but also enhanced the mechanical properties of the silk fibroin sponges. Moreover, the nanocomposite sponges exhibited the absence of the cytotoxicity as well as promoting cell spreading. Thus, all of these results might indicate the potential utility of this nanocomposite system for further exploration as a scaffolding material.

5.6 Acknowledgements

The authors would like to acknowledge Associate Professor Pitt Supaphol for their stimulating discussion. This work was supported in part by the National Research Council of Thailand (through a research grant for ''Multidisciplinary Research Series in Tissue Engineering'' project), Chulalongkorn University (through a research grant from the Ratchadaphisek Somphot Endowment Fund), the Thailand Research Fund (through the Royal Golden Jubilee Ph.D Program i.e., RGJ grant), the Petroleum and Petrochemical Technology Consortium (through a governmental loan from the Asian Development Bank), and the Petroleum and Petrochemical College, Chulalongkorn University. The authors wish to thank Queen Sirikit Sericulture Center (Saraburi Province, Thailand) and Surapon Foods Public Co., Ltd. (Thailand) for supplying essential materials for this study.

5.7 References

[1] Altman GH, Diaz F, Jakuba C, Calabro T,Horan RL, Chen J, Lu H, Richmond J, Kaplan DL. Silk-based biomaterials. Biomaterials 2003;24:401–16.

[2] Wen CM, Ye ST, Zhou LX, Yu Y. Silk-induced asthma in children: a report of 64 cases. Annals Allergy 1990;65:375–8.

[3] Soong HK, Kenyon KR. Adverse reactions to virgin silk sutures in cataract surgery. Ophthalmology 1984;91:479–83.

[4] Meinel L, Hofmann S, Karageorgiou V, Kirker-Head C, McCool J, Gronowicz G, Zichner L, Langer R, Vunjak-Novakovic G, Kaplan DL. The inflammatory responses to silk films in vitro and in vivo. Biomaterials 2005;26:147-55.

[5] Li M, Ogiso M, Minoura N. Enzymatic degradation behavior of porous silk fibroin sheets. Biomaterials 2003;24:357–65.

[6] Arai T, Freddi G, Innocenti C, Tsukada M. Biodegradation of Bombyx mori silk fibroin fibers and films. Journal of Applied Polymer Science 2004;91:2383-90.

[7] Jin H-J, Park J, Karageorgiou V, Kim U, Valluzzi R, Cebe P, Kaplan DL. Water-stable silk films with reduced beta-Sheet content. Advanced Functional Materials 2005;15:1241-47.

[8] Minoura N, Aiba S, Gotoh Y, Tsukada M, Imai Y. Attachment and growth of cultured fibroblast cells on silk protein matrices. Journal of Biomedical Materials Research 1995;29:1215–21.

[9] Unger RE, Peters K, Wolf M, Motta A, Migliaresi C, Kirkpatrick CJ. Endothelialization of a non-woven silk fibroin net for use in tissue engineering: growth and gene regulation of human endothelial cells. Biomaterials 2004;25:5137–46.

[10] Unger RE, Wolf M, Peters K, Motta A, Migliaresi C, Kirkpatrick CJ. Growth of human cells on a non-woven silk fibroin net: a potential for use in tissue engineering. Biomaterials 2004;25:1069–75.

[11] Yamada H, Igarashi Y, Takasu Y, Saito H, Tsubouchi K. Identification of fibroin-derived peptides enhancing the proliferation of cultured human skin fibroblasts. Biomaterials 2004;25:467–72.

[12] Jin H-J, Chen J, Karageorgiou V, Altman GH, Kaplan DL. Human bone marrow stromal cell responses on electrospun silk fibroin mats. Biomaterials 2004;25:1039–47.

[13] Li C, Vepari C, Jin H-J, Kim HJ, Kaplan DL. Electrospun silk-BMP-2 scaffolds for bone tissue engineering. Biomaterials 2006;27:3115–24.

[14] Nam J, Park YH. Morphology of regenerated silk fibroin: effects of freezing temperature, alcohol addition, and molecular weight. Journal of Applied Polymer Science 2001;81:3008-21.

[15] Saitoh H, Ohshima K, Tsubouchi K, Takasu Y, Yamada H. X-ray structural study of noncrystalline regenerated Bombyx mori silk fibroin. International Journal of Biological Macromolecules 2004;34:259-65.

[16] Sumita M, Shizuma T, Miyasaka K, Ishikawa K. Effect of reducible properties of temperature, rate of strain, and filler content on the tensile yield stress of nylon

6 composite filled with ultrafine particles. Journal of Macromolecular Science. Part B, Physics 1983;B22:601-18.

[17] Sumita M, Tsukumo T, Miyasaka K, Ishikawa K. Tensile yield stress of polypropylene composites filled with ultrafine particles. Journal of Materials Science 1983; 18:1758-64.

[18] Morin A, Dufresne A. Nanocomposites of chitin whiskers from Riftia Tubes and poly(caprolactone). Macromolecules 2002;35:2190-99.

[19] Nair KG, Dufresne A. Crab shell chitin whisker reinforced natural rubber nanocomposites. 1. processing and swelling behavior. Biomacromolecules 2003;4:657-65.

[20] Nair KG, Dufresne A. Crab shell chitin whisker reinforced natural rubber nanocomposites. 2. mechanical Behavior. Biomacromolecules 2003;4:666-74.

[21] Nair KG, Dufresne A. Crab shell chitin whisker reinforced natural rubber nanocomposites. 3. effect of chemical modification of chitin whiskers. Biomacromolecules 2003;4:1835-42.

[22] Sriupayo J, Supaphol P, Blackwell J, Rujiravanit R. Preparation and characterization of a chitin whisker-reinforced chitosan nanocomposite films with or without heat treatment. Carbohydrate Polymers 2005;62:130–36.

[23] Sriupayo J, Supaphol P, Blackwell J, Rujiravanit R. Preparation and characterization of alpha-chitin whisker-reinforced poly(vinyl alcohol) nanocomposite films with or without heat treatment. Polymer 2005;46:5637–44.

[24] Howling GI, Dettmar PW, Goddard PA, Hampson FC, Dormish M, Wood EJ. The effect of chitin and chitosan on the proliferation of the human skin fibroblasts and keratinocytes in vitro. Biomaterials 2001;22:2959-66.

[25] Chatelet C, Damour O, Domard A. Influence of the degree of acetylation on some biological properties of chitosan films. Biomaterials 2001;22:261-68.

[26] Wongpanit P, Sanchavanakit N, Pavasant P, Supaphol P, Tokura S, Rujiravanit R. Preparation and characterization of microwave-treated carboxymethyl chitin

and carboxymethyl chitosan films for potential use in wound care application. Macromolecular Bioscience 2005;5:1001–12.

[27] Tomihata K, Ikada Y. In vitro and in vivo degradation of films of chitin and its deacetylated derivatives. Biomaterials 1997;18:567-75.

[28] Marchessault RH, Morehead FF, Walter NM. Liquid crystal systems from fibrillar polysaccharides. Nature 1959;184:632-33.

[29] Lu Y, Wend L, Zhang L. Morphology and properties of soy protein isolate thermoplastics reinforced with chitin whiskers. Biomacromolecules 2004;5:1046-51.

[30] Paillet M, Dufresne A. Chitin whisker reinforced thermoplastic nanocomposites. Macromolecules 2001;34:6527-30.

[31] Baxter A, Dillon M, Taylor KDA, Robert GAF. Improved method for i.r. determination of the degree of N-acetylation of chitosan. International Journal of Biological Macromolecules 1992;17:166-69.

[32] Hokugo A, Takamoto T, Tabata Y. Preparation of hybrid scaffold from fibrin and biodegradable polymer fiber. Biomaterials 2006;27:61–7.

[33] Bunn P, Mottram JT. Manufacture and compression properties of syntactic foams. Composites 1993;24:565-71.

[34] Min B-M, Lee G, Kim SH, Nam YS, Lee TS, Park WH. Electrospinning of silk fibroin nanofibers and its effect on the adhesion and spreading of normal human keratinocytes and fibroblasts in vitro. Biomaterials 2004;25:1289-97.

[35] Lv D, Cao C, Zhang Y, Ma X, Zhu H. Preparation of insoluble fibroin films without methanol treatment. Journal of Applied Polymer Science 2005;96:2168-73.

[36] Kim U, Park J, Kim HJ, Wada M, Kaplan DL. Three-dimensional aqueous-derived biomaterial scaffolds from silk fibroin. Biomaterials 2005;26:2775–85.

[37] Freyman TM, Yannas IV, Gibson LJ. Cellular materials as porous scaffolds for tissue engineering. Progress in Materials Science 2001;46:273-82.

[38] O'Brien FJ, Harley BA, Yannas IV, Gibson L. Influence of freezing rate on pore structure in freeze-dried collagen-GAG scaffolds. Biomaterials 2004;25:1077–86.

[39] Robert GAE. Chitin Chemistry. Hong Kong: Macmillan; 1992:203-67.

[40] Rovel J-F, Marchessaultf RH. In vitro chiral nematic ordering of chitin crystallites. International Journal of Biological Macromolecules 1993;15:329-35.

[41] Magoshi J, Mizuide M, Magoshi Y. Physical properties and structure of silk. VI. Conformational changes in silk fibroin induced by immersion in water at 2 to 130 8C. Journal of Polymer Science: Polymer Physics Edition 1979;17:515-20.

[42] Asakura T, Kuzuhara A, Tabeta R, Saito H. Conformational characterization of Bombyx mori silk fibroin in the solid state by high-frequency carbon-13 cross polarization-magic angle spinning NMR, x-ray diffraction, and infrared spectroscopy. Macromolecules 1985;18:1841-45.

[43] Pearson FG, Marchessault RH, Liang CY. Infrared spectra of crystalline polysaccharide V. chitin. Journal of Polymer Science 1960;43:101-16.

[44] Chen M-H, Chen C-R, Hsu S-H, Sun S-P, Su W-F. Low shrinkage light curable nanocomposite for dental restorative material. Dental Materials 2006;22:138–45.

[45] Deng X, Hao J, Wang C. Preparation and mechanical properties of nanocomposites of poly(D,L-lactide) with Ca-deficient hydroxyapatite nanocrystals. Biomaterials 2001;22:2867-73.

[46] Kim H-W, Kim H-E, Salih V. Stimulation of osteoblast responses to biomimetic nanocomposites of gelatin–hydroxyapatite for tissue engineering scaffolds. Biomaterials 2005;26:5221–30.

[47] Lee JH, Park TG, Park HS, Lee DS, Lee YK, Yoon SC, Nam J-D. Thermal and mechanical characteristics of poly(l-lactic acid) nanocomposite scaffold. Biomaterials 2003;24:2773–8.

[48] Lee YH, Lee JH, An I-G, Kim C, Lee D S, Lee YK, Nam J-D. Electrospun dual-porosity structure and biodegradation morphology of Montmorillonite reinforced PLLA nanocomposite scaffolds. Biomaterials 2005;26:3165–72.

[49] Favier V, Chanzy H, Cavaille JY. Polymer nanocomposites reinforced by cellulose whiskers. Macromolecules 1995;28:6365-7.

[50] Favier V, Canova GR, Shrivastava SC, Cavaille JY. Mechanical percolation in cellulose whisker nanocomposites. Polymer Engineering and Science 1997;37:1732-9.

[51] Valk, P, Pelt AWJ, Busscher HJ, Jong HP, Wildevuur CRH, Arends J. Interaction of fibroblasts and polymer surfaces: relationship between surface free enery and fibroblast spreading. Journal of Biomedical Materials Research 1983;17:807-17.

[52] Ruardy TG, Schakenraad JM, Mei HC, Bussher HJ. Adhesion and spreading of human skin fibroblasts on physicochemically characterized gradient surfaces. Journal of Biomedical Materials Research 1995;29:1415-23.

[53] Qiu Q, Sayer M, Kawaja M, Shen J, Davies JE. Attachment, morphology, and protein expression of rat marrow stromal cells cultured on charged substrate surfaces. Journal of Biomedical Materials Research 1998;42:117-27.

[54] Webb K, Hlady V, Tresco PA. Relationships among cell attachment, spreading, cytoskeletal organization, and migration rate for anchorage-dependant cells on model surfaces. Journal of Biomedical Materials Research 2000;49:362-8.

[55] Schuler M, Owen GR, Hamilton DW, Wild M, Textor M, Brunette DM, Tosatti GP. Biomimetic modification of titatium dental implant model surfaces using the RGDSP-peptide sequence: A cell morphology study. Biomaterials 2006;27:4003-15.

[56] Pelham RJ, Wang YL. Cell locomotion and focal adhesions are regulated by substrate flexibility. Proceedings of the National Academy of Sciences USA 1997;94:13661-5.

[57] Fereol S, Fodil R, Labat B, Galiacy S, Laurent VM, Louis B, Isabey D, Planus E. Sensitivity of alveolar macrophages to substrate mechanical and adhesive properties. Cell Motility and the Cytoskeleton 2006;63:321-40.

Table 5.1 Bulk densities and specific moduli of the methanol-treated chitin whisker/silk fibroin sponges at a various C/S ratios

Methanol-treated sponges at different C/S ratios	Bulk density $(g \cdot cm^{-3}) \times 10^{2}$	Specific modulus $(kPa \cdot g^{-1} \cdot cm^{3}) \times 10^{-2}$
0	1.59±0.071	4.43±0.64
1:8	1.47±0.023	5.00±1.32
2:8	1.54±0.042	11.8±2.40*
4:8	1.88±0.051	33.3±5.21*

* = $P<0.05$; significant against the specific modulus of the neat silk fibroin sponges.

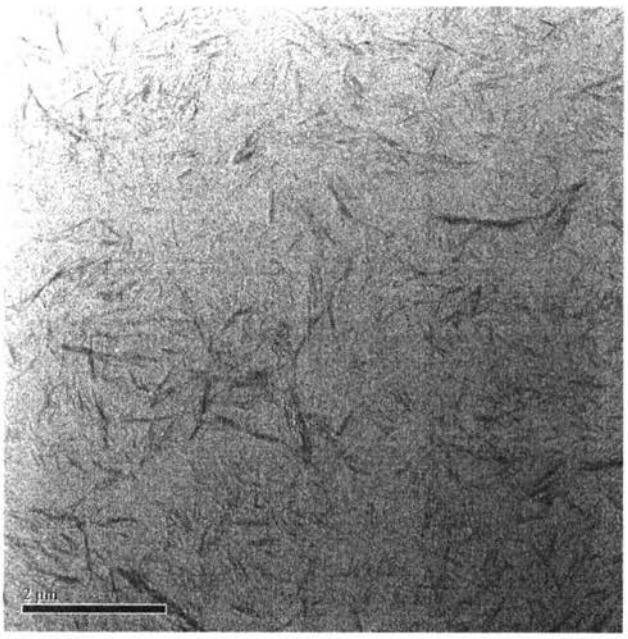

(A)

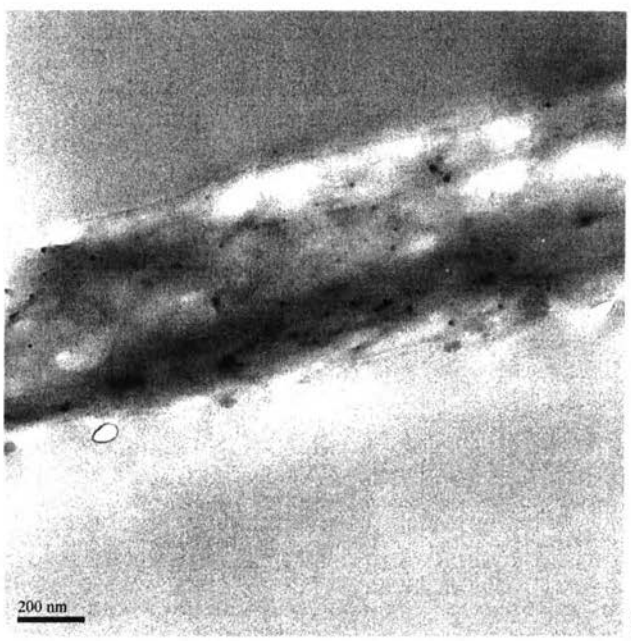

(B)

Figure 5.1 TEM micrographs of chitin whisker; Bar, 2 μm (A), and TEM micrographs of ultrathin section of chitin whisker/silk fibroin sponge at C/S ratios of 4/8; Bar, 200 nm (B).

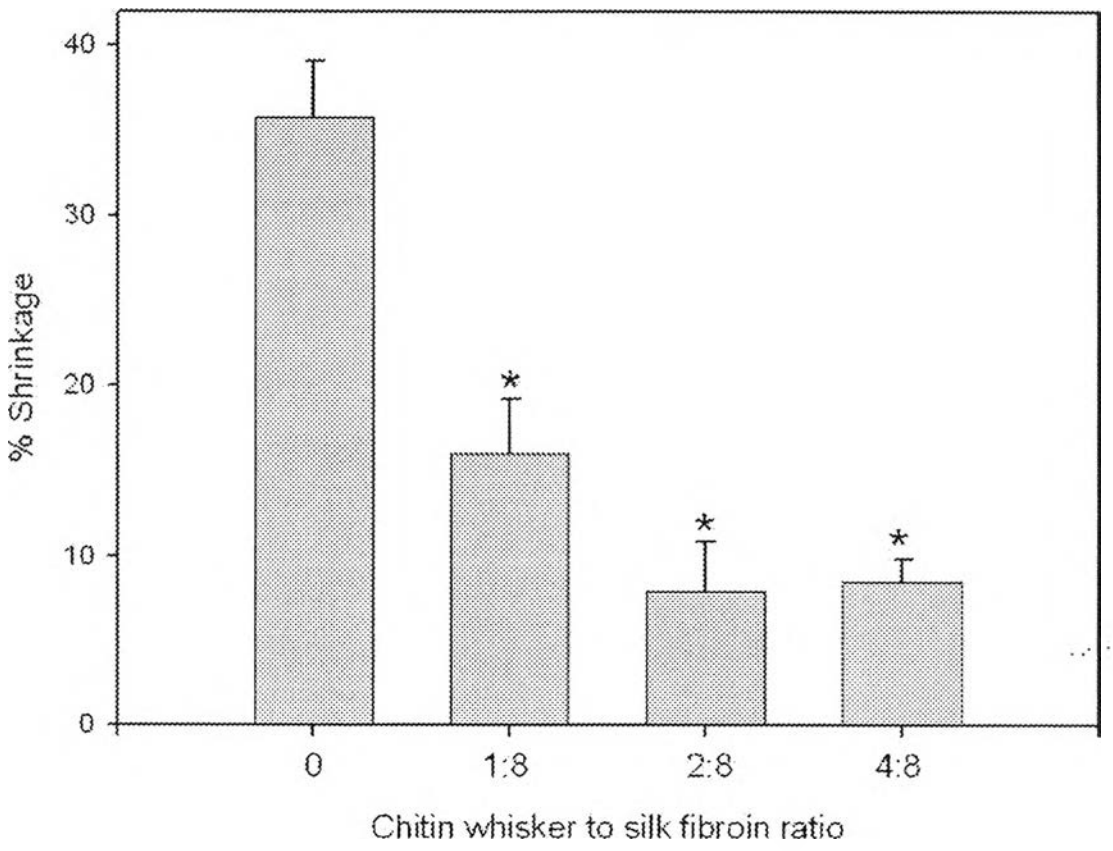

Figure 5.2 Percent shrinkages of chitin whisker/silk fibroin sponges at various C/S ratio. *, $P<0.05$; significant against the percent shrinkage of the neat silk fibroin sponges.

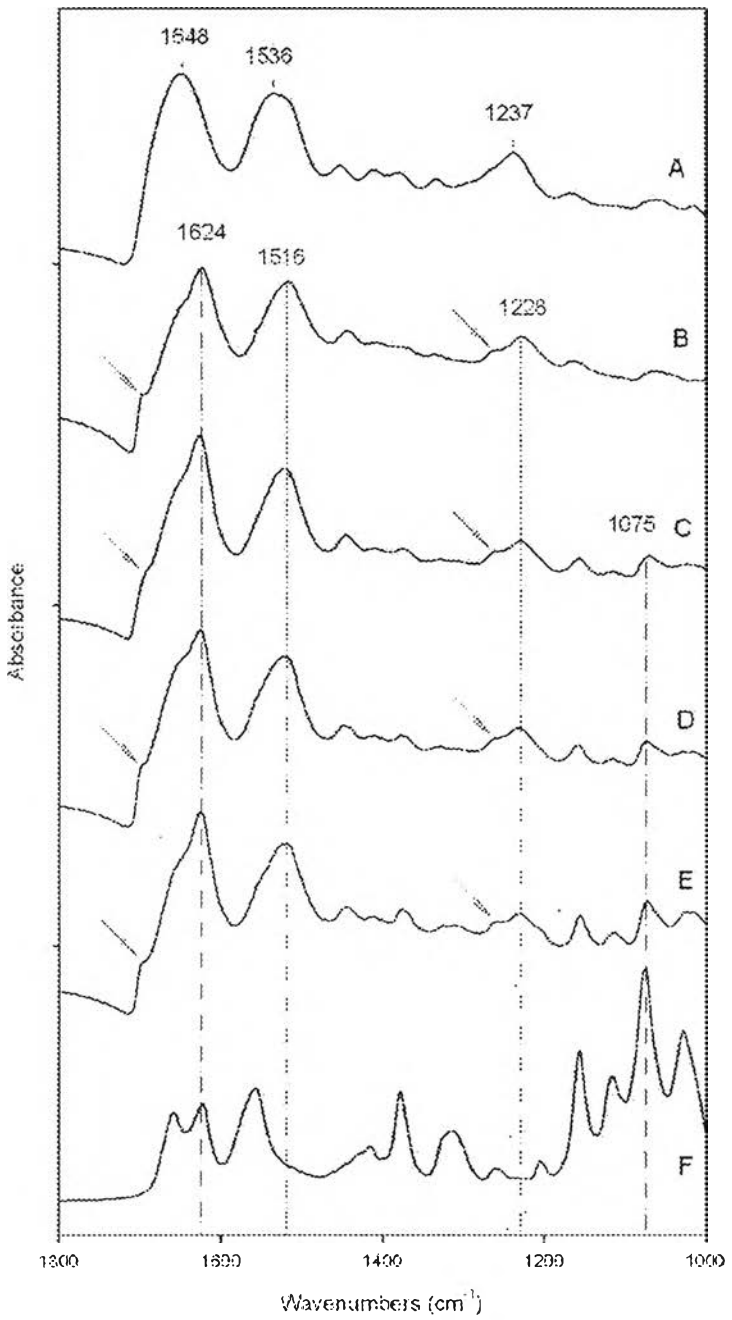

Figure 5.3 FTIR spectra of the as-prepared silk fibroin sponge (A), methanol-treated sponges at various C/S ratios (B to E), and chitin whisker film (F). Arrows indicate the absorption shoulder.

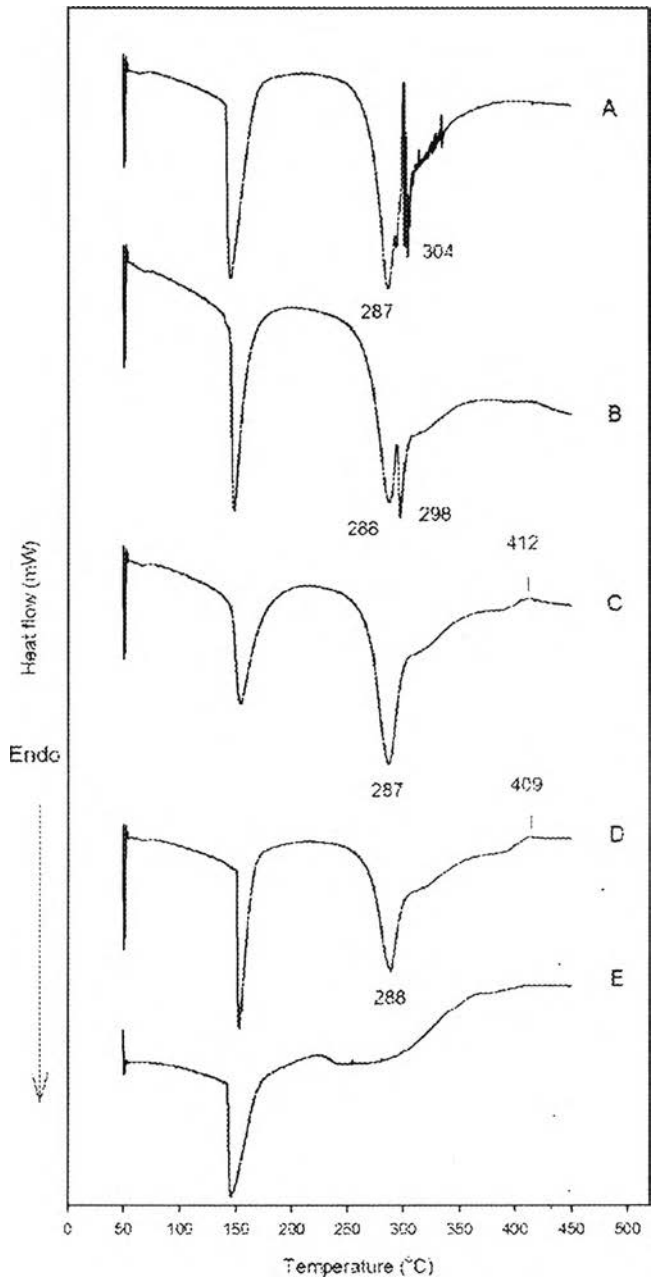

Figure 5.4 DSC thermograms of the methanol-treated silk fibroin sponge (A), the methanol-treated chitin whisker/silk fibroin sponges having different C/S ratios, 1/8 (B), 2/8 (C), 4/8 (D), and the freeze-dried chitin whisker (E).

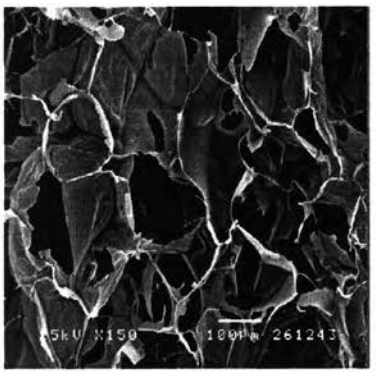
15kV X150
100µm 261243

(A)

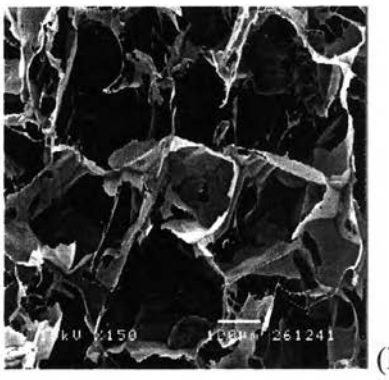
kV X150
100µm 261241

(B)

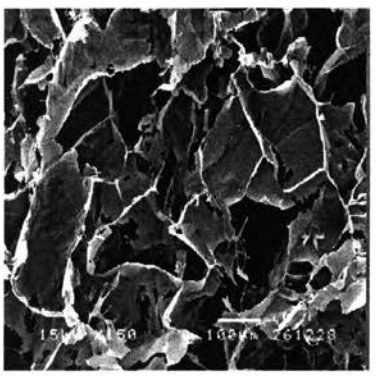
15kV X150
100µm 261228

(C)

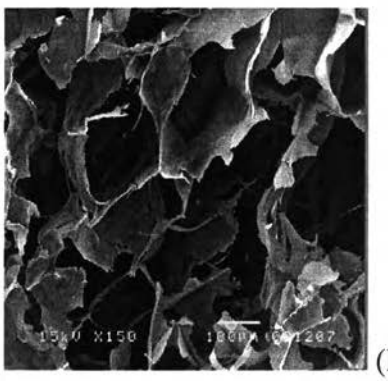
15kV X150

(D)

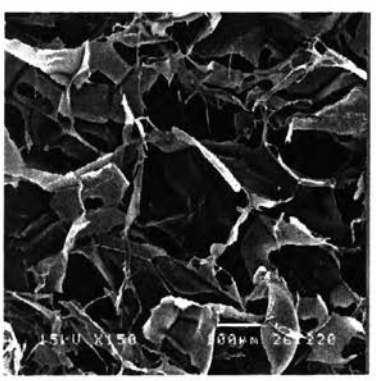
15kV X150
100µm 261220

(E)

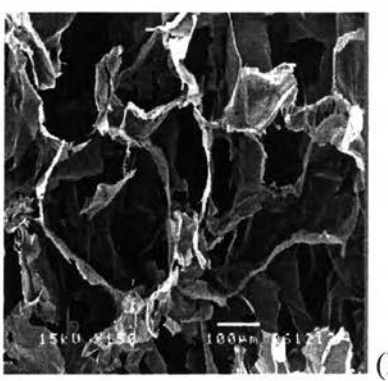
15kV X150
100µm

(F)

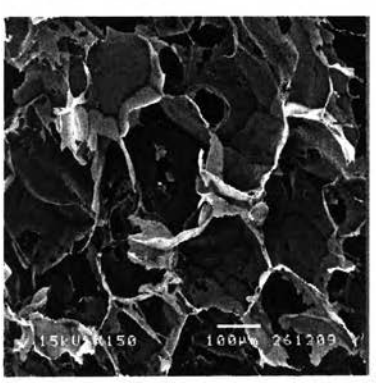
15kV X150
100µm 261209

(G)

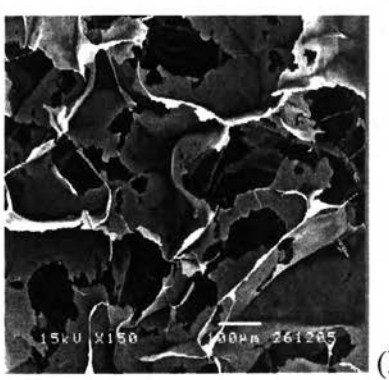
15kV X150
100µm 261205

(H)

Figure 5.5 Cross-sectional SEM micrographs of chitin whisker/silk fibroin sponges at C/S ratio of 0 (A), 1/8 (B), 2/8 (C) or 4/8 (D); And the corresponding methanol-treated sponges at C/S ratio of 0 (E), 1/8 (F), 2/8 (G) or 4/8 (H).

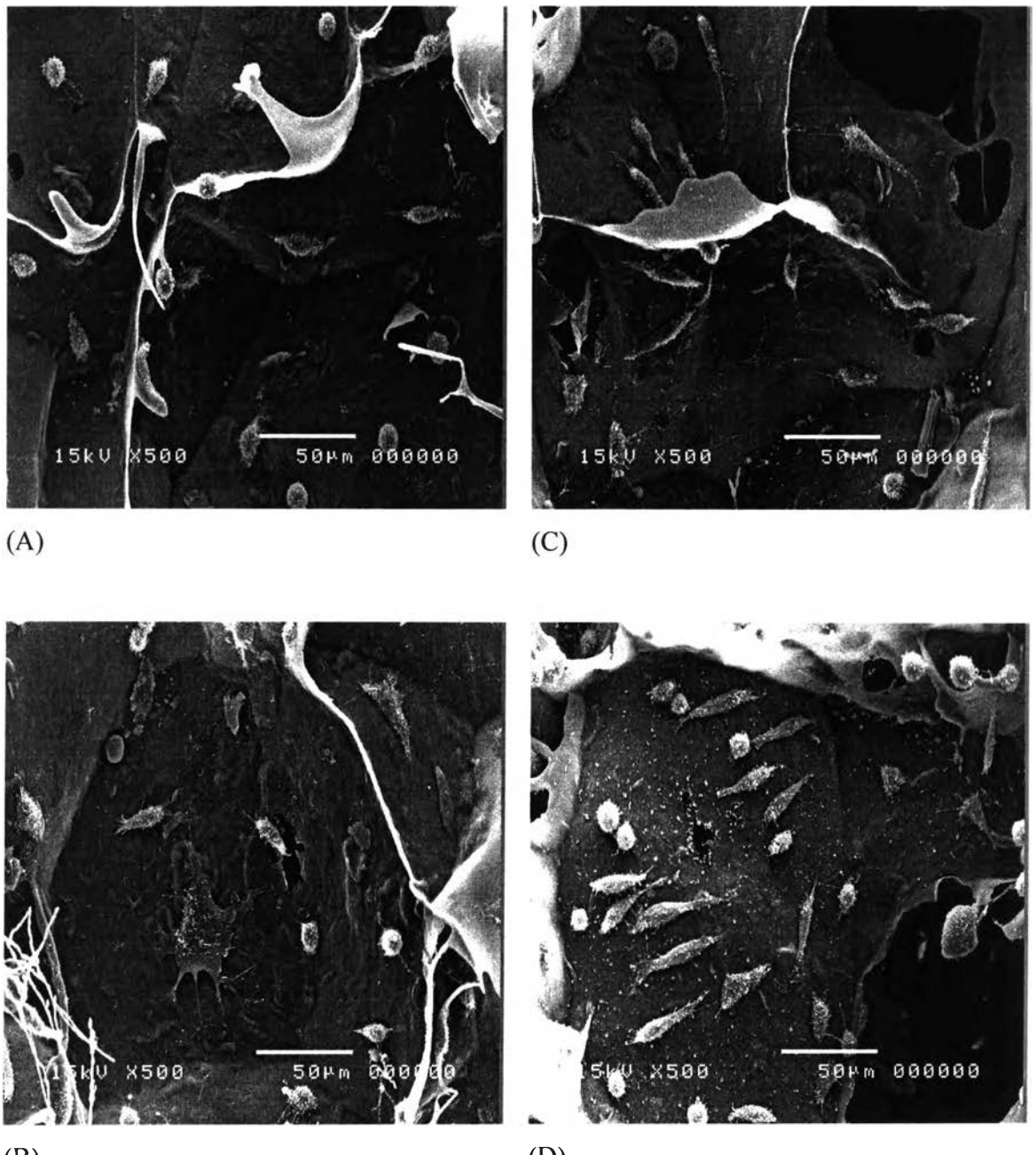

Figure 5.6 SEM micrographs of attached cells on methanol-treated silk fibroin sponges for (A) 6 and (B) 24 h of cultivation and SEM micrographs of attached cells on methanol-treated chitin whisker/silk fibroin sponges at C/S ratio of 4/8 for (C) 6 and (D) 24 h of cultivation.

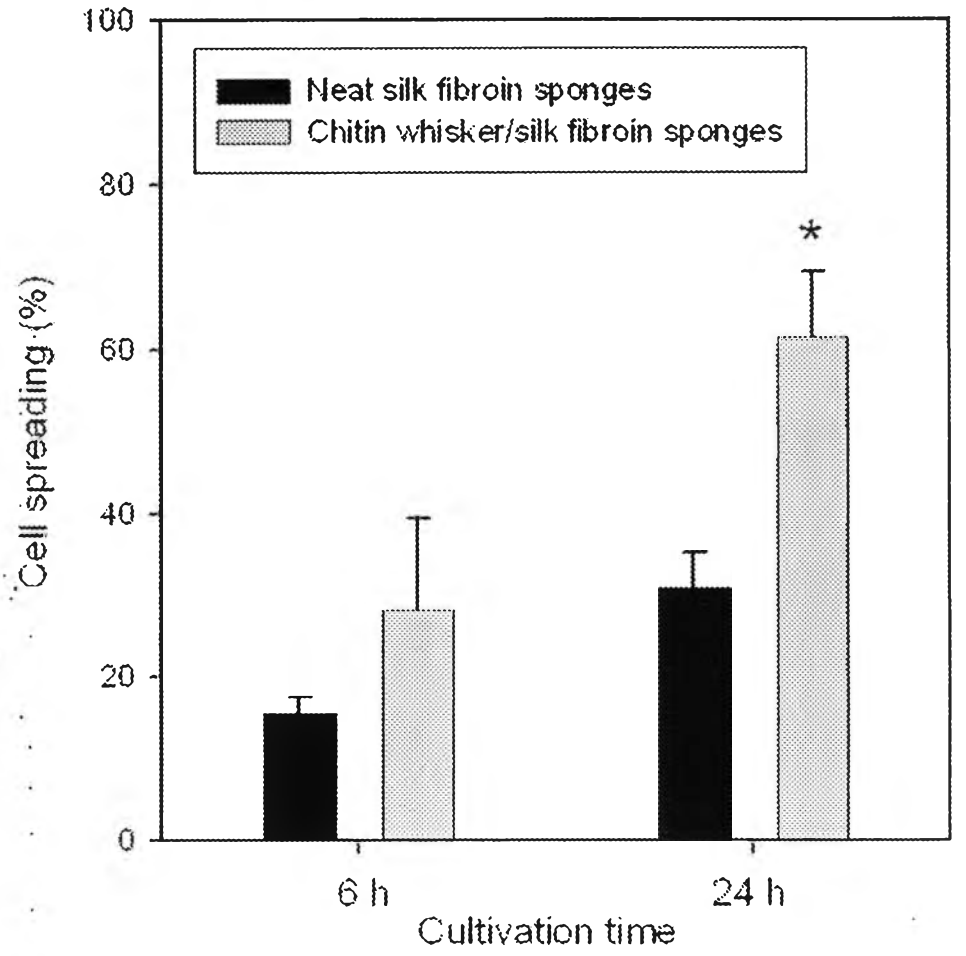

Figure 5.7 Percent cell spreading of the L929 cells on methanol-treated neat silk fibroin sponges and methanol-treated chitin whisker/silk fibroin sponges having C/S ratio at 4:8, *, $P<0.05$; significant against the percent cell spreading of methanol-treated neat silk fibroin sponges.